Article

Hybrid Direction of Arrival Precoding for Multiple Unmanned Aerial Vehicles Aided Non-Orthogonal Multiple Access in 6G Networks

Laura Pierucci [ID]

Department of Information Engineering, University of Florence, 50139 Firenze, Italy; laura.pierucci@unifi.it

Abstract: Unmanned aerial vehicles (UAV) have attracted increasing attention in acting as a relay for effectively improving the coverage and data rate of wireless systems, and according to this vision, they will be integrated in the future sixth generation (6G) cellular network. Non-orthogonal multiple access (NOMA) and mmWave band are planned to support ubiquitous connectivity towards a massive number of users in the 6G and Internet of Things (IOT) contexts. Unfortunately, the wireless terrestrial link between the end-users and the base station (BS) can suffer severe blockage conditions. Instead, UAV relaying can establish a line-of-sight (LoS) connection with high probability due to its flying height. The present paper focuses on a multi-UAV network which supports an uplink (UL) NOMA cellular system. In particular, by operating in the mmWave band, hybrid beamforming architecture is adopted. The MUltiple SIgnal Classification (MUSIC) spectral estimation method is considered at the hybrid beamforming to detect the different direction of arrival (DoA) of each UAV. We newly design the sum-rate maximization problem of the UAV-aided NOMA 6G network specifically for the uplink mmWave transmission. Numerical results point out the better behavior obtained by the use of UAV relays and the MUSIC DoA estimation in the Hybrid mmWave beamforming in terms of achievable sum-rate in comparison to UL NOMA connections without the help of a UAV network.

Keywords: hybrid precoding; millimeter wave; non-orthogonal multiple access scheme; massive MIMO; unmanned aerial vehicles; direction of arrivals (DoA); MUSIC algorithm

1. Introduction

The explosive number of devices demands data traffic growth and new radio spectrum resources in future 6G systems and the IoT context. Key enabling technologies are (i) the underutilized millimeter wave (mmWave) band (between 30 GHz and 300 GHz), which could be valuable for its wide bandwidth and higher spectral efficiency, and (ii) NOMA, which could be valuable for simultaneously supporting multiple users on the same time-frequency resources. The joint use of the large spectrum available in mmWaves together with massive multiple-input-multiple-output (MIMO) strategies allows ultra-high data rates to be guaranteed through spatial directional transmissions compensating for the high propagation loss of mmWaves communications [1]. This directional nature of mmWaves transmissions needs the support of one radio frequency (RF) chain for each user on the same time-frequency resource. Therefore, the hardware complexity and costs of the mmWave MIMO system increase with an increase in the number of users. Hybrid architectures, which combine phase shifters based on analog precoding and digital precoding, reduce the costs practically by selecting a reduced number of RF chains. However, even if hybrid beamforming structures are implemented, the user's channels are highly correlated in mmWave communications, and thus, the users cannot be separated by linear operations. Such a correlation facilitates integration with NOMA technology. NOMA can simultaneously serve multiple users on the same time-frequency resource by converting their channel gains into multiplexed gains in the power domain and by using successive interference cancellation (SIC) at the receiver to remove intra-channel interference with a decoding order based on the channel conditions [2–4].

In the literature, different papers analyze the spectral efficiency (SE) and the energy efficiency (EE) maximization problem mainly for a downlink mmWave MIMO with hybrid beamforming [5,6]. In [3], a power allocation (PA) problem to optimize EE is considered for an uplink NOMA-assisted mmWave MIMO system under users' quality-of-service (QoS) and quality-of-experience requirements [7]. In [4], power allocation and beamforming are jointly considered to maximize the sum rate of a pair of users in a mmWave NOMA system by using an analog beamforming structure indeed of a hybrid mmWave beamforming structure.

Simultaneous wireless information and power transfer (SWIPT) techniques are integrated in mmWave massive MIMO-NOMA systems to maximize the energy efficiency in [8], and consequently, each user can extract both information and energy from the received RF signals by using a power splitting receiver.

In the 6G vision, low Earth orbit (LEO) satellites and diverse aerial platforms, such as UAVs, are considered to support IoT development in remote areas and in emergency situations thanks to the mobility, flexibility and good channel conditions of UAVs. UAVs have been developed for their monitoring capabilities, implemented by on board sensors, for services in agriculture or security border controls. In addition, UAVs are used as a flying base station (BS) to provide ubiquitous connectivity and effectively increase the coverage and throughput of wireless systems through the optimization of UAVs' positions and trajectories [9].

Recently, UAVs have been considered to act as relays for cooperative communications due to the high probability to establish LoS links with the ground terminals. UAV-assisted relaying systems operate according to the two classical types of transmission protocols, namely decode-and-forwarding (DF) and amplify-and-forwarding (AF) [10].

Several papers consider UAV communications combined with orthogonal multiple access (OMA) to maximize the energy efficiency or throughput by optimizing the source/relay transmit power and the UAV speed and trajectory design as, e.g., in [11]. The paper [12] focuses on a UAV full duplex (FD) relay with joint beamforming and power allocation to optimize the instantaneous data rate when the UAV flight follows a circular trajectory. FD relaying allows for a relay node to simultaneously transmit and receive in the same band, unlike half-duplex (HD) mode [10,13]. Therefore, a natural choice is to combine FD relays with NOMA to enhance spectral efficiency.

A UAV-supported clustered-NOMA system for the 6G-enabled IoT is detailed in [14], where the numerous terminals are partitioned into clusters and the UAV provides services to the clusters by using wireless-powered communication (WPC) to optimize the uplink average achievable sum rate of all terminals by designing the UAVs' trajectory.

In [15], a multiple-UAV-aided NOMA scheme is proposed to improve spectral and energy efficiency for cellular uplinks. In particular, half of users are partitioned in clusters served by multiple UAV relays, and the other ones communicate with the BS directly. A location-based user pairing (UP) scheme associates the clustered users with the multiple-UAV-aided NOMA to minimize the resource allocation problem.

However, all the aforementioned works focus on UAV-relay-aided NOMA without considering mmWave communications. The severe signal power attenuation in the mmWave band impacts UAV connectivity performance, especially when very long communications distances exist between the ground users and the associated UAV which serves them.

Therefore, this paper addresses the design of a UAV-enabled FD relaying network in the mmWave band to aid an uplink NOMA cellular system.

In detail, a multiple-UAV-relaying network supports NOMA technology, and hybrid mmWave beamforming is considered at the base station (BS), which can estimate the DoA information of UAVs to improve the overall sum rate of the system. Indeed, the DoAs are unknown and the MUltiple SIgnal Classification (MUSIC) method [16] considered in this paper estimates directly the DoAs at the hybrid mmWave beamformer.

In [17], a beamspace MUSIC algorithm is used to estimate path directions for mmWave channel estimation problem showing that the hybrid precoding structure can avoid the spectrum ambiguity and maximize the number of resolvable path directions. The mmWave

channel estimation problem is also considered in [18] by using MUSIC for the hybrid analog/digital beamformer with 2D co-prime arrays where the directions can be uniquely estimated by finding the common peaks of the 2 decomposed subarrays.

Deep-learning approaches are considered to evaluate the angle-of-arrival (AoA) information in the uplink of an mmWave communication system based on MUSIC to enhance classification accuracy in [19]. The above papers use the MUSIC algorithm to derive the DoA information in mmWave hybrid beamforming, but they do not deploy an UAV-relay network, as in this paper.

To the best of our knowledge, this paper is the first contribution that considers jointly i) the UL mmWave communications, ii) the hybrid beamforming with DoA estimation based on the MUSIC method and iii) multiple UAVs acting as an aerial BS to relay NOMA transmissions and, consequently, achieve better data rate for users who can suffer severe channel conditions. Moreover, a novel maximization design of the overall sum-rate is proposed for the uplink mmWave transmission of the multiple-UAV-relay-aided NOMA 6G system.

The contributions of this paper can be summarized as follows:

- We consider a multiple-UAV-aided NOMA network where each UAV acts as a mobile FD relay in mmWave UL for 6G cellular systems;
- We propose the use of the MUSIC algorithm at the hybrid beamforming to detect the DoA estimations for each UAV and improve the performance of the UAV-aided NOMA cellular system;
- We propose an optimization procedure in order to maximize the average achievable sum rate of the UL mmWave UAV relay network by taking into accounts LoS obstruction, channel time-varying condition, the DoA information at the hybrid beamforming due to the different spatial directions of UAVs, as well as the requirements in terms of quality of service (QoS) for each user.

The paper is organized as follows. Section 2 presents the proposed system model, channel model, the mmWave hybrid beamforming, the MUSIC algorithm and the problem formulation to optimize the global UL sum rate of the UAV-network-aided NOMA cellular system. In Section 3, the numerical results providing a comparison with the NOMA cellular system without the use of multi-UAV relays are shown. Finally, Section 4 concludes the paper and outlines future research activities.

2. System Model and Problem Formulation

A UAV-enabled full-duplex relaying system is considered to aid an uplink mmWave NOMA cellular system consisting in a BS, with N users and K UAVs, as shown in Figure 1. The N users are randomly distributed in the cell of radius R, and the BS is located at the center of the cell.

We assume that the BS is unable to deliver the superimposed signals to the NOMA users in a far subarea of the cell because the link between users and BS is negligible due to severe blockage.

Each UAV acts as a DF relay to help data transmission between the BS and users and operates in FD mode.

We suppose that K UAVs are flying at height H_k in such a way that all links from UAVs to BS are LOS channels. The elevation angles between the BS and the UAVs are denoted as $(\theta_1, \theta_2, ..., \theta_k)$, and $\varphi_{n,k}$ is the elevation angle between the n-th user (named as user equipment UE_n) and UAV_k, as shown in Figure 1.

2.1. Path loss model

The links from ground users and UAV are LOS or no LOS (NLOS) channels due to the presence of buildings, vegetation etc., which can obstruct the signals propagation. In detail, the channel gain between the k-th UAV and the BS is, according to [20–22],

$$\rho_{k,BS} = \zeta_{LOS}(d_{k,BS})^{-\alpha}, \tag{1}$$

and if the UAV_k is in LOS with the $n-th$ user, the channel gain is defined as

$$\rho_{n,k} = \zeta_{LOS}(d_{n,k})^{-\alpha}, \tag{2}$$

where $d_{k,BS}$ and $d_{n,k}$ represent the distances between UAV_k and BS and between UAV_k and UE_n, respectively. ζ_{LOS} denotes the additional attenuation factor of the LOS channel at the reference distance $d_{ref} = 1$ m, and α is the path loss exponent at the air channel. UAVs are in *LOS* with probability $p_{LOS}(d) = \frac{1}{1+Cexp(-(B\varphi_{n,k}-C))}$, where B and C are constants related to the environment, whereas UAVs are in NLOS according to the complementary probability $p_{NLOS}(d) = 1 - p_{LOS}(d)$.
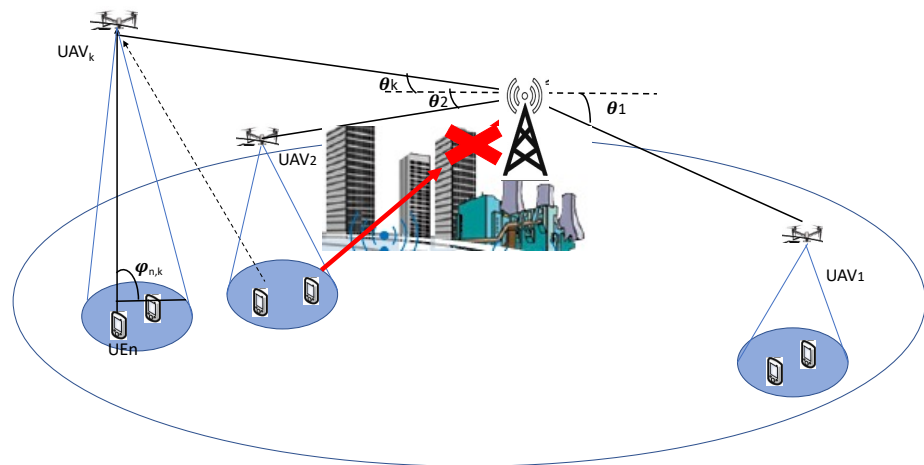

Figure 1. Multiple-UAV-relay-network-aided mmWave NOMA cellular system.

2.2. MmWave Hybrid Beamforming

In mmWave communications, large phase arrays are usually adopted to overcome the high propagation losses, and in combining with NOMA, mmWave beamforming is used to increase beam gain and serve multiple users. Usually, hybrid analog/digital beamforming is adopted in mmWave NOMA communications, where the precoding is performed in hybrid mode by combining the digital baseband precoding with an analog RF beamforming driven by a limited number of RF chains. This hybrid analog/digital beamforming is a cost-effective solution due to the use of massive antennas with limited RF chains. It can be easily implemented through the use of analog phase shifters together with the abilities of digital precoding, which allow the beams to be directed towards the desired user and remove inter-user interferences [23,24].

In particular, we consider the hybrid beamforming architecture at the BS with a number N_{RF} of RF chains exploiting NOMA in each RF chain and spatial division multiple access (SDMA) between RF chains [8], as shown in Figure 2 .

From the angle domain perspective, the knowledge of DoAs plays a fundamental role.

In this paper, the UAVs' angle information are discovered by using the MUSIC algorithm implemented at the hybrid mmWave beamforming. We assume that the number of UAVs does not exceed the number of available RF chains, i.e., $K \leq N_{RF}$.

The received signal at the BS after RF and digital beamforming combining can be expressed as [19,24]

$$\mathbf{y} = \mathbf{D}^H\mathbf{A}^H\mathbf{Hs} + \mathbf{D}^H\mathbf{A}^H\mathbf{w}, \tag{3}$$

where $\mathbf{H}_{N_R \times K}$ is the channel matrix (detailed in Equation (6)), N_R is the number of receiving antennas at the BS, $\mathbf{s}$ denotes the transmit signal, $\mathbf{w}$ is the zero-mean independent and identically distributed (i.i.d.) Gaussian white noise vector with power σ_w^2 and $\mathbf{A}_{N_R \times N_{RF}}$, $\mathbf{D}_{N_{RF} \times K}$ are the analog and digital beamforming matrices (see Equations (4) and (5)), respectively, with $N_{RF} < N_R$.
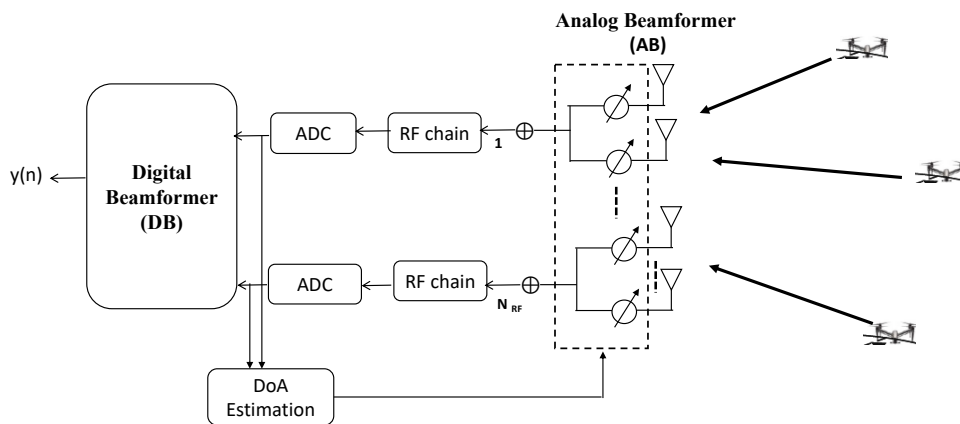
Figure 2. Hybrid mmWave beamformer with DoAs estimation.

In partially-connected hybrid mmWave beamforming, the antenna array with N_R elements can be organized into groups, called subarrays, and each subarray connected to one RF chain processes each received signal by a phase shifter. Then, all of them are added up as shown in Figure 2.

Therefore, the analog matrix $\mathbf{A}_{N_R \times N_{RF}}$ of Equation (3) is a diagonal matrix where

$$v_{A,j} = \frac{1}{\sqrt{N_R}}[e^{j\phi_{j,1}}, e^{j\phi_{j,2}}...e^{j\phi_{j,N_R}}] \tag{4}$$

is the vector of subarray j with $j = 1, ..N_{RF}$; ϕ is chosen from a uniform distribution in the range of $[-\pi/2, \pi/2)$. The RF signal passes through N_{RF} parallel RF chains. It is down-converted and then the digital beamforming operation follows. The zero-forcing scheme can be used as a digital beamformer as

$$\mathbf{D} = (\mathbf{H_A^H H_A})^{-1}\mathbf{H_A^H} \tag{5}$$

where $\mathbf{H_A} = \mathbf{A^H H}$ considers the actual channel matrix $\mathbf{H}$ filtered by the analog beamforming matrix $\mathbf{A}$.

2.3. Channel Model

We consider a ray-tracing channel model widely used in mm-Wave communications with a limited number of L scattering paths, as, due to the spatial sparsity in the mm-wave channel, it is expected that the propagation paths are along a small number of directions [19,25,26].

Therefore, each column of the channel matrix $\mathbf{H}$ is defined as

$$\mathbf{h_k} = \sqrt{\frac{1}{L\rho_{k,BS}}} \sum_{i=1}^{L} g_{k,i}\mathbf{a}(\theta_{k,i}) \tag{6}$$

where $g_{k,i}$ is the complex gain of the i-path due to small-scale fading, $\rho_{k,BS}$ is the path loss between the *BS* and the UAV$_k$ and $\theta_{k,i} \in [-\pi/2, ..., \pi/2]$ is the angle of arrival of the $i - th$ path of the $k - th$ UAV.

Without loss of generality, we assume a uniform linear array (ULA) at the *BS* for simplicity, and the steering vector can be expressed as:

$$\mathbf{a}(\theta_{k,i}) = [1, e^{j\frac{2\pi}{\lambda}lsin(\theta_{k,i})}, ...e^{j(N_R-1)\frac{2\pi}{\lambda}lsin(\theta_{k,i})}] \tag{7}$$

where λ is the signal wavelength, and l is the distance among antenna elements, where $l \leq \lambda/2$.

In the following, we assume that in Equation ((6)) the variations of the channel are only caused by the path gains $g_{k,i}$, and the path angles remain unchanged according to the mmWave channel measurements in [27].

2.4. MUSIC Algorithm

The DoA information is estimated by MUSIC spectral estimation on the filtered version of the received signal, as shown in Figure 2, [19,25,26]. The MUSIC algorithm developed by Schmidt [16] is an eigenstructure-based DOA-finding method and, similar to other parametric algorithms such as ESPRIT, has demonstrated a superior resolution with respect to the non-parametric methods.

By considering a partially connected hybrid mmWave beamforming, after the analog beamforming and the analog-to-digital conversion, the baseband signal is [19,28]:

$$\mathbf{y} = \mathbf{A}^{\mathbf{H}}\mathbf{H}\mathbf{s} + \mathbf{A}^{\mathbf{H}}\mathbf{w} \tag{8}$$

By performing eigenvalue decomposition on the covariance matrix $\mathbf{R_{yy}}$ of the output vector $\mathbf{y}$ of the virtual array, we have:

$$\mathbf{R_{yy}} = E_S \Lambda_S E_S^H + \sigma_w^2 E_w E_w^H$$

where $\mathbf{E_s}$ is the $(N_{RF} \times K)$ matrix of the signal eigenvectors corresponding to the K largest eigenvalues, $\mathbf{E_w}$ is the $(N_{RF} \times (N_{RF} - K))$ noise subspace matrix with eigenvectors corresponding to the smallest $(N_{RF} - K)$ singular values, and $\mathbf{\Lambda_s}$ is the $(K \times K)$ diagonal matrix containing the K largest eigenvalues $\lambda_1 > \lambda_2, ... > \lambda_K$ of $\mathbf{R}_{yy}$. It is clear that the signal subspace E_s and the noise subspace E_w are orthogonal.

The MUSIC algorithm utilizes the orthogonality between the two complementary spaces to estimate the spatial signal. Therefore, the DoA estimation $\hat{\theta}_k$ consists of finding the values of θ, whereby the filtered vector $Aa_D(\theta)$ is related to the signal subspace of $\mathbf{R}_{yy}$, where

$$\mathbf{a_D}(\theta) = \frac{1}{\sqrt{N_R}}[1, e^{j\frac{2\pi}{\lambda}lsin(\theta)}, ...e^{j\frac{2\pi}{\lambda}(N_R-1)lsin(\theta)}]$$

is the array manifold vector of the virtual array.

By using the definition of a pseudo-spectrum of the MUSIC algorithm, the estimated DoA of the emitter direction can be calculated by maximizing the function

$$P_{MU}(\hat{\theta}) = \frac{1}{\mathbf{a_D^H}(\theta)\mathbf{A}\mathbf{E_w}\mathbf{E_w^H}\mathbf{A^H}\mathbf{a_D}(\theta)}, \tag{9}$$

which provides high resolution of angle separation.

2.5. Problem Formulation

Considering the NOMA method in each beam, intra-beam superposition coding at the transmitter and SIC at the receiver are performed. In the case of uplink mmWave NOMA, the users begin to transmit uplink signals x_1 and x_2 at the same time and in the same frequency band. For the proposed multiple-UAV relay network shown in Figure 1, each UAV decodes the mixed signals of the two users in its beam (called, for example, UE_1 and UE_2) and then transmits the superimposed signal $\mathbf{s}$ to the BS according to

$$\mathbf{s} = \sqrt{\mathbf{P_1}}\hat{x}_1 + \sqrt{\mathbf{P_2}}\hat{x}_2, \tag{10}$$

where $\hat{x}_1$ and $\hat{x}_2$ are the decoded signals of UE_1 and UE_2, respectively, and $\mathbb{E}[|\hat{x}_1|^2] = \mathbb{E}[|\hat{x}_2|^2] = 1$ and $P_1 + P_2$ cannot exceed the maximum transmission power of the UAV.

In the conventional NOMA with a single-antenna, usually the information of the user with a lower channel gain is decoded first to maximize the sum rate. In contrast, in mmWave NOMA, the decoding order depends on both channel gain and beamforming gain. Without loss of generality, assuming that UE_1 has a better channel condition with respect to UE_2 in the area covered by UAV_k [4,29], the achievable rates are

$$R_1 = log_2(1 + \frac{|\mathbf{h_1^H U}|^2 P_1}{|\mathbf{h_2^H U}|^2 P_2 + \sigma_k^2}) \tag{11}$$

$$R_2 = log_2(1 + \frac{|\mathbf{h_2^H U}|^2 P_2}{\sigma_k^2}), \tag{12}$$

and the achievable rate from UAV_k is

$$R_{UAV_k} = log_2(1 + \frac{|\mathbf{h_k^H W}|^2 P_{UAV_k}}{\sigma_w^2}), \tag{13}$$

where P_1, P_2 and P_{UAV_k} are the transmission power of UE_1, UE_2 and UAV_k respectively, $\mathbf{h_1}$, $\mathbf{h_2}$ are the channel response vector between the UE_1, UE_2 and UAV_k, $\mathbf{h_k}$ is the channel response vector between the UAV_k and the BS, $\mathbf{U}$ and $\mathbf{W}$ represent jointly the analog and digital precoding matrices at the UAV_k and at the BS, whereas σ_k^2 and σ_w^2 are the power of the zero-mean additive Gaussian white noise at the UAV_k and BS, respectively.

Therefore, the available rate received at the BS considering the UAV_k acting as a relay is

$$R_{sum} = min(R_1 + R_2, R_{UAV_k}). \tag{14}$$

To maximize the uplink average achievable sum rate of all terminals of the multiple-UAV-aided NOMA mmWave system by dynamically tracking the DoAs of multiple UAVs, the optimization problem can be formulated as

$$\begin{aligned} \underset{\theta_k}{\text{Maximize}} \quad & \sum_{k=1}^{K} R_{sum} \\ s.t. \quad & \\ & R_1 \geq \tilde{r} \\ & R_2 \geq \tilde{r} \\ & R_{sum} \geq \tilde{r} \\ & P_1 + P_2 \leq P_{UAV_k} \\ & P_{UAV_1} + P_{UAV_2} + \dots P_{UAV_k} \leq P \end{aligned} \tag{15}$$

where $\tilde{r}$ denotes the minimal data rate constraint for each user and the last constraint indicates the transmitted power constraint with P being the maximum total transmitted power.

This optimization problem is very complicated to be solved directly because the problem is non-convex and may not be converted to a convex problem with simple manipulations. Consequently, in order to validate the effectiveness of the proposed optimization problem and the accuracy of the derived analytical model, we resort to numerical simulations.

3. Simulation Results

In this section, we evaluate the performance of the proposed network of multiple UAV relays supporting the uplink mmWave NOMA system. In the considered system, UAV relays are located in different positions with different spatial directions with respect to the BS, and hybrid mmWave beamforming with MUSIC technique is adopted to derive the different DoAs in order to optimize the achievable uplink sum-rate. In detail, we simulate three different scenarios, i.e., an UL mmWave NOMA without a UAV network, a single UAV and a network of multiple UAVs supporting the UL mmWave NOMA. The cellular

network has an area of 300×300 m^2 with the BS located in the center. A total of 32 users are randomly and uniformly distributed in this area.

The BS is equipped with an ULA of $N_R = 64$ antennas and $N_{RF} = 4$ RF chains to simultaneously serve a number K of UAVs with $K \leq N_{RF}$. The UAVs deployed in the cell have different DoAs at the BS uniformly distributed between $[-\pi/2, \, ... \, \pi/2]$, and each UAV covers a pair of users who have poor connections with the BS due to a severe blockage condition. The UAV has $N_{UR} = 16$ receiving antennas which transmits towards the BS with one antenna.

We choose to associate the considered blocked user pair not to the closest UAV in term of distance, but to the one offering the best communication performance, as especially in a very dense urban scenario, the nearest available UAV may be in NLOS visibility. An accurate DoA estimation at the BS can monitor the fluctuations of the UAV motion and consequently improve the performance of the overall uplink sum rate.

The main parameters for an urban scenario are summarized in Table 1 [20,27].

Table 1. Simulation parameters.

Number of users	N = 32
Number of UAVs	K = 4
Urban LOS probability parameters	C = 9.6117, B = 0.1581
The additional attenuation factor for LOS channel	$\zeta_{LOS} = 10^{-6.14}$
The additional attenuation factor for NLOS channel	$\zeta_{NLOS} = 10^{-7.2}$
The path loss exponent	$\alpha_{LOS} = 2 \; \alpha_{NLOS} = 2.92$
UAV deployment height H	[100–300] m
UAV transmit power	$P_{UAV} = 20$ dBm
User transmit power	$P_{UE} = 10$ dBm
Minimal rate constraint for users	$\tilde{r} = 3$ bps/Hz

In Figure 3, the achievable sum rate is shown in terms of the varying signal-to-noise ratio (SNR) for the multi-UAV network with respect to a single UAV scheme in the case of an LOS environment. The multi-UAV scheme outperforms the single UAV scheme even for low SNR values, as the channels from users to each UAV are in LOS in these simulations realizations and consequently demand low power to transmit towards the UAV.

In the same figure, the case of a multi-UAV scheme without DoA information acquisition is highlighted to validate the performance of the MUSIC method. Indeed, the DoA estimation error is an important problem due to the UAV mobility and dynamic channel variations. However, a more accurate DoA estimation occurs when the UAV is far from the BS [30], and in particular the use of the MUSIC technique allows both the DoA and received powers to be estimated more accurately with respect to other methods [19,24,31].

Figure 4 shows the achievable sum rate results with respect to SNR when multiple UAVs are considered for both the case of LOS and NLOS environments. The MUSIC method at the BS to acquire the DoA information of the UAVs is used. In these simulation results, the heights of UAVs are not considered too high, because even if the links have a higher probability to be in LOS, the impact of the increased distance between the pair of users and the serving UAV decreases the overall link budget, and the links can have a worse SNR. The results are compared with the performance of the UL NOMA mmWave system without the multi-UAV network, i.e, the users can communicate directly by NOMA mmWave link to the BS. The NOMA mmWave link to BS is considered only for evaluating the performance comparison as, practically, the user pair covered by each UAV has a severe blockage and cannot communicate with the BS. The achievable sum rate of the multiple-

UAV network achieves a considerably better performance than the direct NOMA mmWave connection, as shown in Figure 4, providing a improvement of about 6 dB for high SNR values.
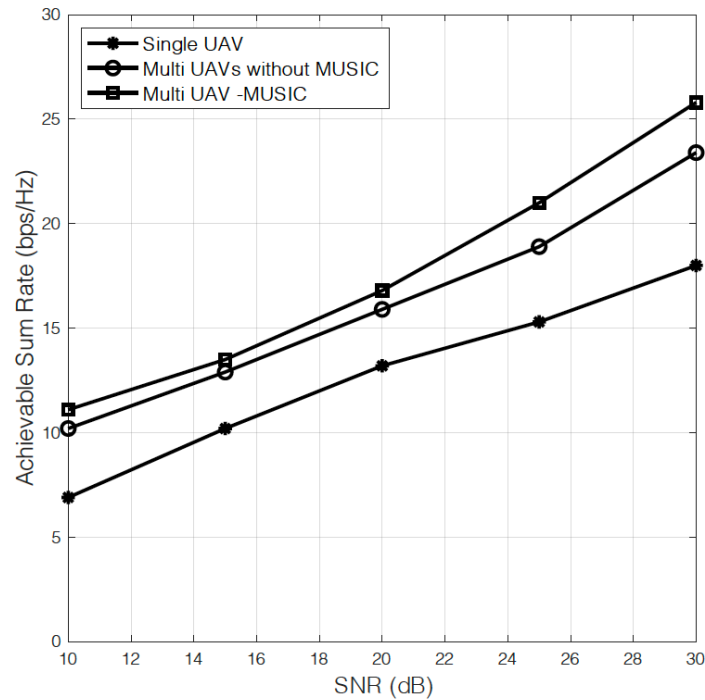
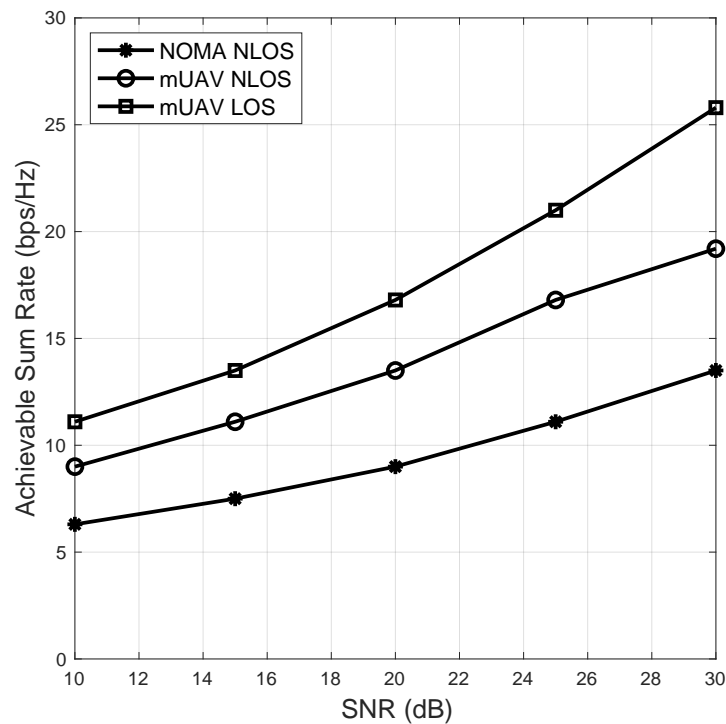**Figure 3.** Achievable rate for multiple UAVs and a single UAV in LOS environment.

Figure 4. Comparison between multi-UAV-aided NOMA and terrestrial NOMA cellular systems.

4. Conclusions

The paper proposes a multi-UAV network where each UAV, acting as a relay, carries out the NOMA method for users experiencing severe blocking to the BS in mmWave com-

munications. Hybrid beamforming architecture is commonly combined with mmWave transmission. We have investigated how the angle of arrival information can be estimated by the MUSIC technique performed after the analog part and the analog-to-digital conversion in the hybrid beamformer to derive the DoA of each UAV. The estimation of DoAs allows the specific antenna multi-beam targeting to be formed to each UAV. This provides an intrinsic mitigation of the UAV fluctuation effects, enhancing the UL signal reception, and leads to the substantial improvement of the system sum rate, as confirmed by simulation results. We have investigated the problem of how to maximize the sum rate of the multiple-UAV-aided NOMA mmWave system, where each pair of users is served by an UAV and where we need to find the hybrid beamforming vector to steer towards each UAV. MUSIC allows DoAs and received power to be estimated more accurately. This results in the enhanced overall sum rate (close to 50%) of the multiple-UAV-aided NOMA network with respect to the NOMA cellular system without the UAV network. In the future, research should investigate minimizing the energy consumption of a multi-UAV network by discovering efficient power associations of ground users with UAV trajectories.

Institutional Review Board Statement: Not applicable.

Informed Consent Statement: Not Applicable

Conflicts of Interest: The author declares no conflict of interest.

References

1. Busari, S.A.; Huq, K.M.S.; Mumtaz, S.; Dai, L.; Rodriguez, J. Millimeter-Wave Massive MIMO Communication for Future Wireless Systems: A Survey. *IEEE Commun. Surv. Tutor.* **2018**, *20*, 836–869. doi:10.1109/COMST.2017.2787460.
2. Ding, Z.; Lei, X.; Karagiannidis, G.K.; Schober, R.; Yuan, J.; Bhargava, V.K. A Survey on Non-Orthogonal Multiple Access for 5G Networks: Research Challenges and Future Trends. *IEEE J. Sel. Areas Commun.* **2017**, *35*, 2181–2195. doi:10.1109/JSAC.2017.2725519.
3. Zeng, M.; Hao, W.; Dobre, O.A.; Poor, H.V. Energy-Efficient Power Allocation in Uplink mmWave Massive MIMO With NOMA. *IEEE Trans. Veh. Technol.* **2019**, *68*, 3000–3004. doi:10.1109/TVT.2019.2891062.
4. Xiao, Z.; Zhu, L.; Choi, J.; Xia, P.; Xia, X. Joint Power Allocation and Beamforming for Non-Orthogonal Multiple Access (NOMA) in 5G Millimeter Wave Communications. *IEEE Trans. Wirel. Commun.* **2018**, *17*, 2961–2974. doi:10.1109/TWC.2018.2804953.
5. Wang, B.; Dai, L.; Wang, Z.; Ge, N.; Zhou, S. Spectrum and Energy-Efficient Beamspace MIMO-NOMA for Millimeter-Wave Communications Using Lens Antenna Array. *IEEE J. Sel. Areas Commun.* **2017**, *35*, 2370–2382. doi:10.1109/JSAC.2017.2725878.
6. Fang, F.; Zhang, H.; Cheng, J.; Leung, V.C.M. Energy-Efficient Resource Allocation for Downlink Non-Orthogonal Multiple Access Network. *IEEE Trans. Commun.* **2016**, *64*, 3722–3732. doi:10.1109/TCOMM.2016.2594759.
7. Pierucci, L. The quality of experience perspective toward 5G technology. *IEEE Wirel. Commun.* **2015**, *22*, 10–16. doi:10.1109/MWC.2015.7224722.
8. Dai, L.; Wang, B.; Peng, M.; Chen, S. Hybrid Precoding-Based Millimeter-Wave Massive MIMO-NOMA With Simultaneous Wireless Information and Power Transfer. *IEEE J. Sel. Areas Commun.* **2019**, *37*, 131–141. doi:10.1109/JSAC.2018.2872364.
9. Masaracchia, A.; Nguyen, L.D.; Duong, T.Q.; Yin, C.; Dobre, O.A.; Garcia-Palacios, E. Energy-Efficient and Throughput Fair Resource Allocation for TS-NOMA UAV-Assisted Communications. *IEEE Trans. Commun.* **2020**, *68*, 7156–7169. doi:10.1109/TCOMM.2020.3014939.
10. Simoni, R.; Jamali, V.; Zlatanov, N.; Schober, R.; Pierucci, L.; Fantacci, R. Buffer-Aided Diamond Relay Network With Block Fading and Inter-Relay Interference. *IEEE Trans. Wirel. Commun.* **2016**, *15*, 7357–7372. doi:10.1109/TWC.2016.2601333.
11. Zeng, Y.; Zhang, R.; Lim, T.J. Throughput Maximization for UAV-Enabled Mobile Relaying Systems. *IEEE Trans. Commun.* **2016**, *64*, 4983–4996. doi:10.1109/TCOMM.2016.2611512.
12. Song, Q.; Zheng, F.; Zeng, Y.; Zhang, J. Joint Beamforming and Power Allocation for UAV-Enabled Full-Duplex Relay. *IEEE Trans. Veh. Technol.* **2019**, *68*, 1657–1671. doi:10.1109/TVT.2018.2889349.
13. Chiti, F.; Fantacci, R.; Pierucci, L. Energy Efficient Communications for Reliable IoT Multicast 5G/Satellite Services. *Future Internet* **2019**, *11*, 164. doi:10.3390/fi11080164.
14. Na, Z.; Liu, Y.; Shi, J.; Liu, C.; Gao, Z. UAV-supported Clustered NOMA for 6G-enabled Internet of Things: Trajectory Planning and Resource Allocation. *IEEE Internet Things J.* **2020**. doi:10.1109/JIOT.2020.3004432.
15. Wang, J.; Liu, M.; Sun, J.; Gui, G.; Gacanin, H.; Sari, H.; Adachi, F. Multiple Unmanned-Aerial-Vehicles Deployment and User Pairing for Nonorthogonal Multiple Access Schemes. *IEEE Internet Things J.* **2021**, *8*, 1883–1895. doi:10.1109/JIOT.2020.3015702.
16. Schmidt, R. Multiple emitter location and signal parameter estimation. *IEEE Trans. Antennas Propag.* **1986**, *34*, 276–280. doi:10.1109/TAP.1986.1143830.

17. Guo, Z.; Wang, X.; Heng, W. Millimeter-Wave Channel Estimation Based on 2-D Beamspace MUSIC Method. *IEEE Trans. Wirel. Commun.* **2017**, *16*, 5384–5394. doi:10.1109/TWC.2017.2710049.

18. Shufeng, L.; Guangjing, C.; Libiao, J.; Hongda, W. Channel estimation based on the PSS-MUSIC for millimeter-wave MIMO systems equipped with co-prime arrays. *EURASIP J. Wirel. Commun. Netw.* **2020**, *17*, 17. doi:10.1186/s13638-020-1637-4.

19. Antón-Haro, C.; Mestre, X. Learning and Data-Driven Beam Selection for mmWave Communications: An Angle of Arrival-Based Approach. *IEEE Access* **2019**, *7*, 20404–20415.

20. Boschiero, M.; Giordani, M.; Polese, M.; Zorzi, M. Coverage Analysis of UAVs in Millimeter Wave Networks: A Stochastic Geometry Approach. In Proceedings of the 2020 International Wireless Communications and Mobile Computing (IWCMC), Limassol, Cyprus, 15–19 June 2020; pp. 351–357. doi:10.1109/IWCMC48107.2020.9148550.

21. Xue, Z.; Wang, J.; Ding, G.; Wu, Q.; Lin, Y.; Tsiftsis, T.A. Device-to-Device Communications Underlying UAV-Supported Social Networking. *IEEE Access* **2018**, *6*, 34488–34502. doi:10.1109/ACCESS.2018.2849440.

22. Andrews, J.G.; Bai, T.; Kulkarni, M.N.; Alkhateeb, A.; Gupta, A.K.; Heath, R.W. Modeling and Analyzing Millimeter Wave Cellular Systems. *IEEE Trans. Commun.* **2017**, *65*, 403–430. doi:10.1109/TCOMM.2016.2618794.

23. Lialios, D.I.; Ntetsikas, N.; Paschaloudis, K.D.; Zekios, C.L.; Georgakopoulos, S.V.; Kyriacou, G.A. Design of True Time Delay Millimeter Wave Beamformers for 5G Multibeam Phased Arrays. *Electronics* **2020**, *9*, 1331. doi:10.3390/electronics9081331.

24. Shu, F.; Qin, Y.; Liu, T.; Gui, L.; Zhang, Y.; Li, J.; Han, Z. Low-Complexity and High-Resolution DOA Estimation for Hybrid Analog and Digital Massive MIMO Receive Array. *IEEE Trans. Commun.* **2018**, *66*, 2487–2501. doi:10.1109/TCOMM.2018.2805803.

25. Khawaja, W.; Ozdemir, O.; Guvenc, I. UAV Air-to-Ground Channel Characterization for mmWave Systems. In Proceedings of the 2017 IEEE 86th Vehicular Technology Conference (VTC-Fall), Toronto, ON, Canada, 24–27 September 2017; pp. 1–5. doi:10.1109/VTCFall.2017.8288376.

26. Alkhateeb, A.; El Ayach, O.; Leus, G.; Heath, R.W. Channel Estimation and Hybrid Precoding for Millimeter Wave Cellular Systems. *IEEE J. Sel. Top. Signal Processing* **2014**, *8*, 831–846. doi:10.1109/JSTSP.2014.2334278.

27. Akdeniz, M.R.; Liu, Y.; Samimi, M.K.; Sun, S.; Rangan, S.; Rappaport, T.S.; Erkip, E. Millimeter Wave Channel Modeling and Cellular Capacity Evaluation. *IEEE J. Sel. Areas Commun.* **2014**, *32*, 1164–1179. doi:10.1109/JSAC.2014.2328154.

28. Trigka, M.; Mavrokefalidis, C.; Berberidis K. Full snapshot reconstruction in hybrid architecture antenna arrays. *J. Wirel. Com Netw.* **2020**, *2020*, 243. doi:10.1186/s13638-020-01863-6.

29. Souto, V.; D. Souza, R.; Uchôa-Filho, B. Tx-Rx Initial Access and Power Allocation for Uplink NOMA-mmWave Communications. In *xxxviii Simpósio Brasileiro de Telecom. e Process. de Sinais*; Sociedade Brasileira de Telecom Brazil, 2020.

30. Miao, W.; Luo, C.; Min, G.; Wu, L.; Zhao, T.; Mi, Y. Position-Based Beamforming Design for UAV Communications in LTE Networks. In Proceedings of the ICC 2019—2019 IEEE International Conference on Communications (ICC), Shanghai, China, 15 July 2019; pp. 1–6. doi:10.1109/ICC.2019.8761505.

31. Dastgahian, M.S.; Ghomash, H.K. MUSIC-based approaches for hybrid millimeter-wave channel estimation. In Proceedings of the 2016 8th International Symposium on Telecommunications (IST), Tehran, Iran, 27–28 September 2016; pp. 266–271. doi:10.1109/ISTEL.2016.7881823.